The Structure - Inhibitory Activity Relationships Study in a Series of Cyclooxygenase-2 Inhibitors: A Combined Electronic-Topological and Neural Networks Approach

A. Dimoglo[*,1,2], V. Kovalishyn[3], N. Shvets[1,4] and V. Ahsen[1]

[1]*Gebze Institute of Technology, PK-141, Gebze/Kocaeli, 41400, Turkey*

[2]*Department of Quantum Chemistry, Institute of Chemistry, Kishinev, 2028, Moldova*

[3]*Institute of Bioorganic & Petroleum Chemistry, Kiev, 253660, Ukraine*

[4]*Institute of Mathematics, Academy of Sciences of Moldova, Kishinev, 2028, Moldova*

Abstract. Structure-activity relationships study was performed for a few series of cyclooxygenase-2 (COX-2) inhibitors by using the Electronic-Topological Method combined with Neural Networks (ETM-NN). Specific molecular fragments were found for active compounds ('activity features') from both series by the ETM application. After this, a system of prognosis was developed as the result of training Kohonen's self-organizing maps (SOM) by the fragments. From the detailed analysis of all compounds under study, requirements necessary for a compound to be COX-2 inhibitor were formulated. The analysis showed that any requirements violation for a molecule resulted in a considerable decrease or even complete loss of its activity. The found activity features identified correctly different marketed drugs and new compounds that had passed pre-clinical and clinical trials; this fact confirms the workability of the system developed for the COX-2 inhibitory activity prediction.

Keywords: COX-2 inhibitors, structure-activity relationships, electronic-topological method, neural networks.

INTRODUCTION

All known anti-inflammatory, anti-pyretic and analgesic preparations belonging to the class of non-steroidal anti-inflammatory drags (NSAIDs) were studied enormously from experimental (chemical and pharmacological) point of view [1-3 and references therein], as well as from theoretical one (docking, Monte Carlo simulations [4, 5] etc.). Literature and patent analysis showed that a few thousands of active compounds being potent NSAIDs had been synthesized up to date already. All published works aimed at synthesis and clinical trials of NSAIDs with minor side effects [6, 7] such as ulcer of stomach and GI, internal bleedings, kidney pathology etc., in comparison with other drugs. NSAIDs inhibit prostaglandin synthesis by blocking the cyclooxygenation of arachidonic acid to prostaglandin.

Until recently, a single cyclooxygenase (COX) enzyme was thought to be responsible for metabolic reactions that occur by the prostaglandin synthesis. Now it is known that two isozymes, COX-1 and COX-2, exist, and COX-2 is an inducible form that causes different side effects [7]. In this way, the goal of new searches is to increase the NSAIDs efficiency and selectivity. Some widely used marketed drugs (indomethacyne, ibuprofen, diclofenac, *et al*.) have a high potency in COX-2 inhibiting but insufficient selectivity; others (celecoxib, valdecoxib, refecoxib, etc.), on the contrary, have high selectivity but low inhibition potency [8].

*Address correspondence to this author at the Gebze Institute of Technology, PK-141, Gebze/Kocaeli, 41400, Turkey; Tel: +90 262 653 84 97; Fax: +90 262 653 84 90; E-mail: dimoglo@gyte.edu.tr

The most interesting point is that NSAIDs possess quite distinct structures. Also, their characteristics such as molecular shape, lipophilicity, electron density, flexibility, polarity and H-bonding dynamics allow a wide range of diversity. At the same time, minor modifications to a particular compound are capable of inducing a drastic change in its COX selectivity. A great many publications has arisen recently on the synthesis of COX-2 inhibitors as well as their structure-activity relationships (SAR)investigations. It is worth to mention some of these works that have been devoted to the theoretical study of mechanism of COX-2 inhibition and to the search for the correlation between their structures and inhibitory activity.

The mechanism of different NSAIDs binding to the cyclooxygenase COX-2 active site has been studied in ref. [9] by means of a wide range of theoretical techniques including molecular dynamics and free energy calculations. It was concluded that the theoretical methods predict accurately the binding of different drugs based on different scaffolds. The calculations allowed to describe in detail the key recognition sites and to analyze how these recognition sites change depending on the scaffold of the drug. The conclusion is that the recognition site of COX-2 is very flexible and can adapt its structure to very subtle structural changes in the drug.

Molecular models of the complex between the selective COX-2 inhibitor nimesulide and the cyclooxygenase active site of human prostaglandin-endoperoxide synthase-2 have been built using a combination of homology modelling, conformational searching and automated docking techniques [10]. The stability of the resulting complexes has been assessed by molecular dynamics simulations and interaction energy decomposition. It is found that nimesulide exploits

1389-5575/05 $50.00+.00

the extra space made available by the replacement at position 523 of an isoleucine residue in COX-1 by a valine in COX-2 and establishes electrostatic interactions with both Arg-106 and Arg-499 (Arg-120 and Arg-513, in PGHS-1 numbering). Two alternate binding modes are proposed, which are compatible with the pharmacological profile of this agent as a COX-2 selective inhibitor.

Recently a set of thirty five molecules of 1,3-diarylisoindole derivatives endowed with selective COX-2 inhibitory activity was studied by using comparative molecular field and comparative molecular similarity indices analyses [11, 12]. This work provided useful information regarding the pharmacophoric requirements for the COX-2 inhibitory activity. The FlexX program was used to find out the binding orientation of this new class of 1,3-diaryl isoindoles in the active site of COX-2. Additionally, the flexible docking of eighty two structurally diverse COX-2 inhibitors has been successfully carried out. Simple linear regression analysis provided the correlation coefficient values of 0.73 and 0.67 for the two classes of COX-2 inhibitors.

The *de novo* design program Skelgen has been used in [13] to design COX-2 inhibitor structures for four targets of pharmaceutical interest. It is shown that the Skelgen algorithm generates representatives of many inhibitor classes within a very short time, and that a new similarity measure implemented in the program is useful for comparing and clustering designed structures. Design of new selective COX-2 inhibitors by assembling dynamically molecular building blocks (DycoBlock system) has been proposed by Zhu *et al*. [14]. This method is based on the multiple-copy stochastic dynamics simulation in the presence of a receptor molecule. In this method, a novel algorithm was used to dynamically assemble the molecular building blocks to form candidate compounds. Thus, thirty-three kinds of molecular building blocks were used in the design of novel inhibitors and the investigation of diversity.

With the aim of elucidating structural features that govern the differential inhibitory binding behavior of COX-1 and COX-2 inhibitors, molecular modeling studies were undertaken to generate atomic models compatible with the experimental data available [15]. Manual docking of different COX-2 inhibitors, including selective and non-selective ligands such as rofecoxib, ketoprofen, suprofen, carprofen, zomepirac, indomethacin, diclofenac and meclofenamic acid, was undertaken, followed by using the AMBER program, to refine the structure of the protein ligand complex.

Very recently, the novel molecular alignment method with the Hopfield Neural Network (HNN) was proposed and investigated on a data set of COX-2 inhibitors by applying to the three-dimensional quantitative structure-activity relationship (3D-QSAR) analysis [16]. By this, the molecules were represented by four kinds of chemical properties (hydrophobic group, hydrogen-bonding acceptor, hydrogen-bonding donor, and hydrogen-bonding donor/acceptor), and then the properties of any two molecules were looked upon their correlation by using HNN. Two data sets (inhibitors of human epidermal growth factor receptor-2 and inhibitors of cyclooxygenase-2) were investigated to validate the method. As a result, the robust and predictive 3D-QSAR models were successfully obtained for both data sets. And, finally, there are the most recent studies [17-29] devoted to the synthesis and SAR study in a few new series of COX-2 selective inhibitors.

The goal of the present study is the search of the most potent and selective inhibitors of COX-2 by applying the combination of our own electronic-topological method (ETM) and neural networks (ETM-NNs**)**. Both of them have already been successfully applied but separately to a wide enough variety of tasks related to the structure-activity relationships (SAR) investigation [28-34].

Previously [35], with the help of the ETM, a large series of NSAIDs (192 molecules) belonging to different structural classes and possessing different levels of COX-2 inhibitory activity were studied. The system for the activity prediction developed as the result of this study included 6 pharmacophores, 6 anti-pharmacophores, and conditions necessary for the activity demonstration by a compound, as well. The system is capable of identifying active compounds with high enough probability (~0.96 in average) under condition that compounds with $IC_{50} \leq 0.1$ μM are considered as active ones while for inactive compounds $IC_{50} \geq 2.0$ μM. An examining set of 29 compounds was taken to test the system. It should be mentioned that in the set there were a few skeletons that did not enter the training set. However, the results of that study were in agreement with experimental data on biological activities for all tested compounds.

This work extends the study of various COX-2 inhibitors by applying a new combined approach based on the further analysis of the ETM results by means of Artificial Neural Networks (ANNs). The latter are capable of elucidating structure-activity relationships (SAR) because of their ability to take into account any non-linear dependencies among the values of different molecular characteristics. Therefore, ANNs can be of significant interest for QSAR studies [36]. As an example, the feed-forward neural networks (FFNN) trained with the back propagation algorithm [37, 38] are widely used to perform different chemical calculations. If the dependencies between analyzed descriptors and molecular parameters are non-linear, the neural networks can produce more accurate models than linear regression methods do. This can be very important for practical applications, e.g. such as design of new compounds.

MATERIALS AND METHOD

The Method's Description

Since details of the ETM can be found in literature [39-42], we only give here the most distinguished properties of the ETM relative to other methods used in diverse SAR studies. ETM belongs to the so-called structural methods. So, the main part of the method is a language for the compound structure description. The language reflects the discrete nature of compounds that are viewed as consisting of atoms some of which are chemically bonded. Labelled graphs appeared to be the most appropriate mathematical counterparts of chemical structures and relationships on their atoms and bonds. As known, a graph's representative is a matrix of the order *n x n*, where n is the number of the graph's vertices. Therefore, the ETM proposes Electronic-Topological Matrices of Contiguity (ETMC) to be its own, very special language, for chemical compounds' description. Bonds have no orientation, thus the matrices are

symmetrical relative to their left diagonal, and it is enough to have only the right upper triangle of any such matrix along with its diagonal.

Vertices of such graphs (diagonal elements a_{ii} of the ETMCs) are naturally labeled by values being atomic characteristics (charges, HOMO/LUMO coefficients etc.). For off-diagonal elements there are two possibilities. If they represent chemical bonds, then a fixed bond characteristic is to be chosen for all of them. Otherwise, a value of corresponding distance for the given pair of atoms is taken. To begin the electronic-topological study, one must have a series of compounds that is representative enough (at least, a few tens of substances). The activity of compounds can be estimated either qualitatively (i.e. active/inactive, in which case there are two classes for comparison) or quantitatively (then there can be more than two classes). Ideally, half of compounds in the teaching set should be inactive. After all these conditions have been met, the main steps of the ETM-study can be described as follows:

1. Calculation of spatial and electron characteristics for atoms and bonds for all compounds under study.
2. The ETMC formation for every molecular structure, by choosing previously appropriate atom and bond properties from the data calculated (usually, they are charges for atoms being the diagonal elements and the Wiberg's indices for bonds; otherwise, distances are taken for non-bonded atoms).
3. Setting on some desirable level for the activity prediction and some precision values to have ability to compare the values of corresponding atomic and bond characteristics.
4. Comparing all ETMCs with the ETMC for the most active compound, to select those structural fragments $\mathbf{S_i}$ (i I), which are common for all active compounds only.
5. Estimating the fragments selected ("activity features") in accordance with probabilistic criterion ($\mathbf{P_a}$) and choosing those of them, which correspond to the desired level of prediction that has been set before calculations. If the fragments found are not informative enough, change some initial settings (or all of them) and repeat steps 3-5.

When the activity features $\mathbf{S_i}$, i I, have been successfully found for a teaching set and subsequently proved for an examining set, they can be used to predict the activity of interest (**A**) for new series of compounds with probability $\mathbf{P_a}$ estimated previously for each structural feature.

A criteria that are commonly used in structural methods for evaluating the probability of a structural feature $\mathbf{S_i}$ (for a fixed *i*) occurrence in active compounds from the given series are calculated according to the equations

$$\mathbf{P_a} = (n_1+1)/(n_1+n_3+2) \text{ and} \quad (1)$$

$$\alpha_a = \frac{(n_1 \cdot n_4 \cdot n_2 \cdot n_3)}{\sqrt{N_1 \cdot N_2 \cdot N_3 \cdot N_4}} \quad (2)$$

There n_1 and n_2 are amounts of molecules possessing and not possessing the feature of activity $\mathbf{S_i}$ in the class of active compounds, respectively; n_3 and n_4 have the same meaning relative to the class of inactive compounds; N_1 and N_2 are numbers of molecules in the classes of active and inactive compounds, respectively, whereas $N_3 = n_1 + n_3$ and $N_4 = n_2 + n_4$. The probability value $\mathbf{P_a}$ is related exactly to the compounds that contain an activity feature found from the ETM calculations, while $\alpha_{\mathbf{a}}$ takes into account all compounds in the series, as it can be seen from the equations.

As far as the order of an ETMC depends on the number of atoms of the corresponding molecule, ETMCs cannot be used in a straightforward manner as the input for ANNs. Consequently, the information contained in ETMCs should be rearranged somehow in order to serve as input vectors of equal dimensionality for an ANN. To overcome this problem, a special algorithm being a combination of FFNN and the Kohonen's self-organizing map (SOM) [43, 44] has been proposed. The supervised learning was performed using a variant of FFNN known as the Associative Neural Network (ASNN) [45]. This type of networks improves the prediction ability of FFNN by explicit correction of the bias of this method.

The Kohonen SOM training is carried out in such manner, that input vectors from the n-dimensional space (n>>2), which possess similar properties are mapped to the same neuron or some nearby neurons in the two-dimensional space. Therefore, by considering all input vectors projected to the same output neuron, it is possible to determine clusters of vectors that have similar properties in the n-dimensional space. Since all vectors from the same cluster are similar, only one of them can be used to represent the properties of all the rest vectors of this cluster. The use of one such vector instead of a number of vectors provides the input data compression. Such compression was used in the current study to align molecules and decrease the number of input parameters used for the ASNNs training (Fig. **1**).

Thus, the principal idea of this new approach is to determine initially for each molecule the number of clusters containing elements of its ETMC, and, afterwards, to use the averaged values of each cluster for the ASNNs training. The algorithm proposed for supervised training makes it possible to evaluate the weights of fragments represented by the ETMC's submatrices (or ETSC, for short) that have been obtained by the ETM calculations. To do this, their projections on the Kohonen's maps that correspond to their initial ETMCs are calculated. In this way the degree of each fragment's presence in a molecule can be determined. This approach by several orders decreases the number of input parameters required for neural network training, preserves the spatial structural information of molecules and calculates neural network models with high generalization ability.

The Scheme of the Combined ETM-NNs Approach

The algorithm for the data resulting from the ETM calculations analysis (ETM-data) is developed on the base of Volume Learning Algorithm created for the analysis of CoMFA data [46]. This method is implemented as a recurrent iterative application of the Kohonen SOMs and ASNNs. The general block-schema of the ETM-NNs data analysis is presented in (Fig. **2**.)

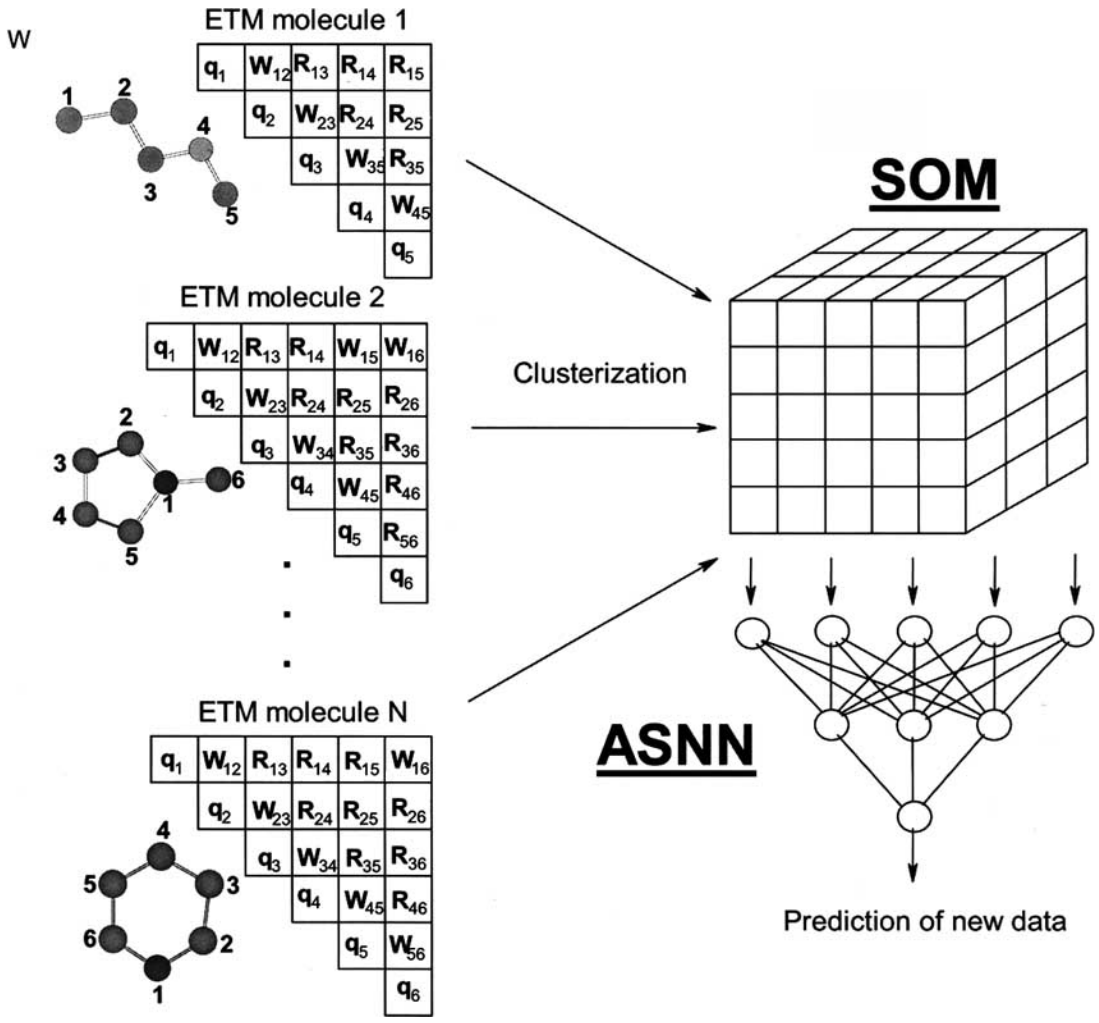

Fig. (1). General scheme of data analysis provided by the ETM-NN method application.

By this approach, the stepwise process of the ETM-data analysis can be summarized as follows:

(1) The initial set of input data formation (ETMCs rearrangement, for all molecules).

(2) The Kohonen's network parameters initialization; calculating clusters from each ETMC, for all molecules.

(3) Data compression by using cluster centers as the initial set.

(4) Analysis of the compressed data by using ASNNs; calculation of the average prediction error (*Ec*).

(5) Comparing the *Ec* value to that one in the preceding stage of learning, *Ep* (initially, *Ep* = 10e-3). If *Ec* < *Ep*, the current cluster distribution is saved.

(6) Decreasing the size of the Kohonen's map.

(7) Repeating the steps 2 – 6 until the map size, *S*, decreases to eight nodes (the number of nodes in a columns (*x*) is 4, the number of rows (*y*) is 2).

(8) Choosing the best cluster distribution, relative to the minimal *E* value, and predicting the activity of new compounds.

(9) The ETMC fragments calculation and the input data set formation for the Kohonen SOM.

(10) Calculation of projections on the units of the Kohonen's SOM for each fragment and the projection error (*Eq*).

(11) The weight of each fragment (1/*Eq*) calculation and new data set creation by using calculated fragment weights as parameters.

(12) Choosing the most informative ETMC fragments (after the ASNN training) by using special pruning methods [47, 48].

(13) Predicting activities of new compounds.

The first step is to prepare an initial data set for the SOM algorithm training (we can call it "triples calculation"). The data sample is a triple (d_1, d_2, d_3), where d_1 and d_2 are charges of two atoms and d_3 is a connection between them (see Fig. **1**). The d_i values, i=1,2,3, are taken from the ETMCs. The total number of data samples corresponds to the amount of all two-atom connections taken from all ETMCs.

The second step includes initialization and training of the Kohonen's network of the size $S=x*y$ (Fig. **2**). The initial

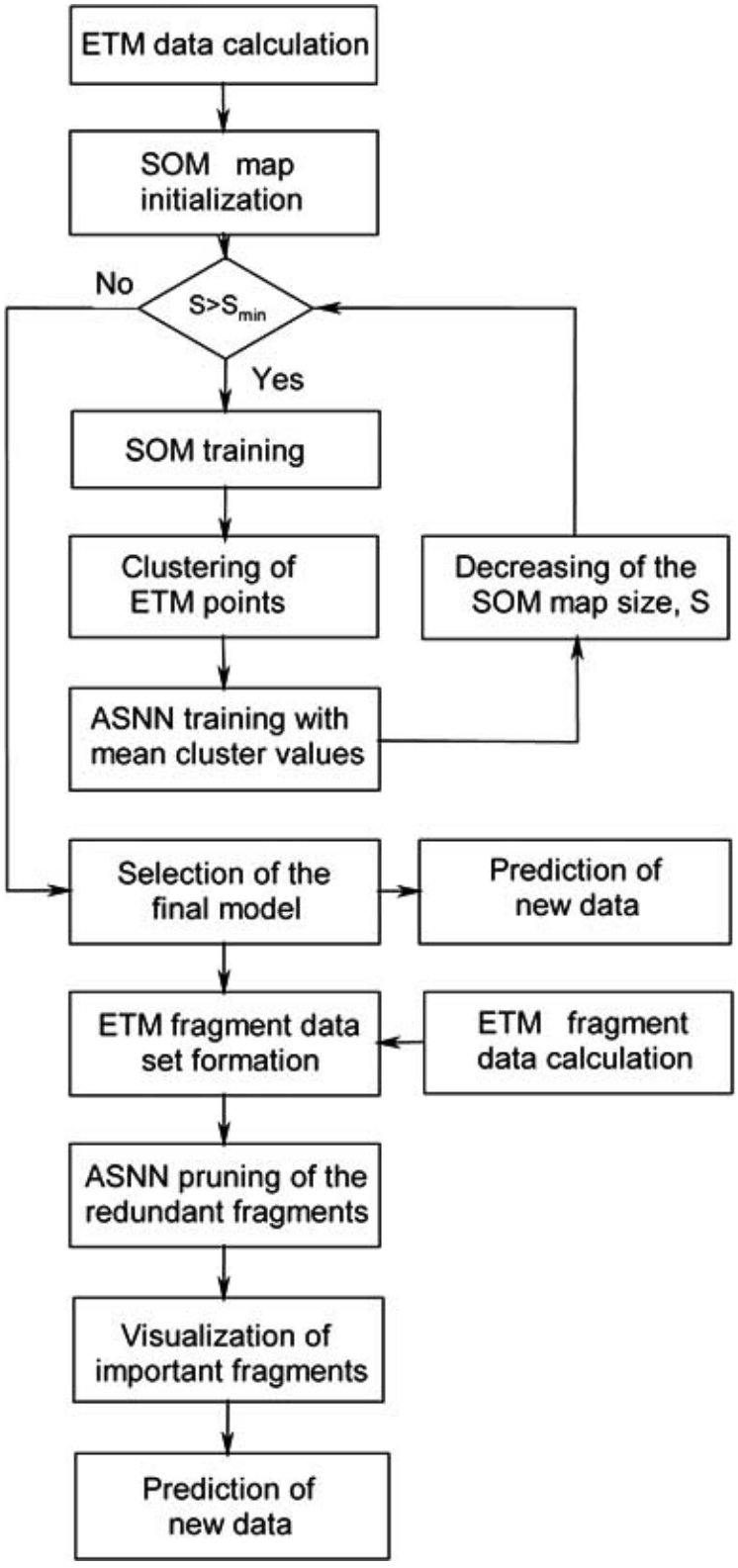

Fig. (2). Block-scheme of the ETM-NN calculations.

size of Kohonen's maps was $S=2*S_{ETM}$, with S_{ETM} being the size of the largest ETM matrix. Upon subsequent compressions, the map size was decreased by two units in both x and y directions. When using the Kohonen's networks, it is possible to create a nonlinear projection of high-dimensional data set onto a low-dimensional domain. Detailed description of a Kohonen's network can be found in [43, 46].

In short, to train a Kohonen's map, two phases are needed. The first phase of 50,000 iterations was used for the

weight vectors of the map neurons for rough ordering. In the second phase with 100,000 iterations, the values of the weight vectors were fine-tuned. The initial learning rate and neighborhood radius of the SOM under training were selected to be α_1=0.6, $\sigma_1=2/5(x\ y)^{0.5}$ and α_2=0.15, $\sigma_2=2/5\sigma_1$ for the first and the second phase, respectively.

To form a compressed sample data set, the cluster centers (C_n) were calculated by averaging over all values entering into the given cluster, $C_n = X_{ni}/m$, where X_{ni} was the value of the *i*-th element of the ETMC for the *n*-th molecule, and *m* was the number of ETMC values entering into the cluster for the molecule *n*.

At the third step, the compressed data are tested on the three-layer ASNNs. A new data set is formed for the ASNN learning from the mean values of input parameters calculated for each cluster (see [45] for details). The number of neurons in the input layer corresponds to the number of clusters obtained as the output of the SOM. The hidden layer contains five neurons. The bias neuron is presented both on the input and hidden layer. An ensemble of *M*=100 neural networks was trained. The activity values were calculated for each network (ASNN) and averaged over all *M* networks. This value was used to calculate the statistical coefficients [49]. The quality of each final model was assessed by the leave-one-out method (LOO). By the method, each molecule is removed from the training set, and the remaining set is used to separate molecules into classes of activity, thereby predicting the activity of this molecule and evaluating the quality of the decision rule.

The fourth step includes the pharmacophores calculations as the ETMCs fragments. At the fifth step, the weight of each fragment (pharmacophore or antipharmacophore) is estimated for each compound as its projection error, *Eq*, relative to the same nodes of the Kohonen's map as its comprising ETMC. The weight is taken as the inverse of its *Eq*: $W_{ij}=1/Eq_{ij}$. Here *i* is the molecule's number, and *j* is the fragment's number. Based on the weight coefficients calculated, a new table was formed that used the fragment weights as parameters.

The last step includes application of the pruning algorithms aiming in a set of the most relevant ETMC fragments selection. The optimized fragments were used to visualize those regions of molecules under study that were found to be important for the analyzed activity demonstration by the molecules.

DATA SETS

Conformational and electronic parameters were calculated for 79 inhibitors of COX-2 taken from different series [50-56]. Biological activities of these compounds were measured on human COX-2 (in the whole cell and/or whole blood assays) and, for some of them, correlated with measurements on the rat paw edema assay. To have the most representative activity fragments as pharmacophores and antipharmacophores (being the result of the ETM calculations), compounds with some very high and, correspondingly, very low values of IC_{50} (substance concentration sufficient for inhibiting 50% of the enzyme) were selected. Next, the compounds were divided into five series by the type of their base skeletons (see Fig. **3**). Tables **1** and **2** contain data on the structures and corresponding values of IC_{50} for all compounds in these series. We shall refer the series of 79 compounds as data set 1, or, in short, DS1, elsewhere below.

All compounds are divided into two classes of highly active (48 mol., IC_{50} < 10 μM) and inactive molecules (31 mol., IC_{50} > 10 μM). Compounds that have been studied previously by the ETM approach [35], are added to our initial sample as well. They are benzopyrane derivatives [57], sulfonyl-containing terphenyls [58], diaryl derivatives of pyrazole [59], and diaryl-substituted pyridines [60] (see Fig. **4**, skeletons VI-IX). Details on the structure of these compounds were reported earlier [35]. The compounds affiliation to different structural classes is very important for our study, so as the fact that related experimental data (biological parameters) are obtained by the same research group [57-60]. At the same time, the search for common pharmacophores in the structures of active compounds is more informative when they possess diverse skeletons but not the similar ones. So, the total number of compounds investigated at the training phase as data set 2, or DS2, is 227. The test set included each tenth selected compound (22 in all).

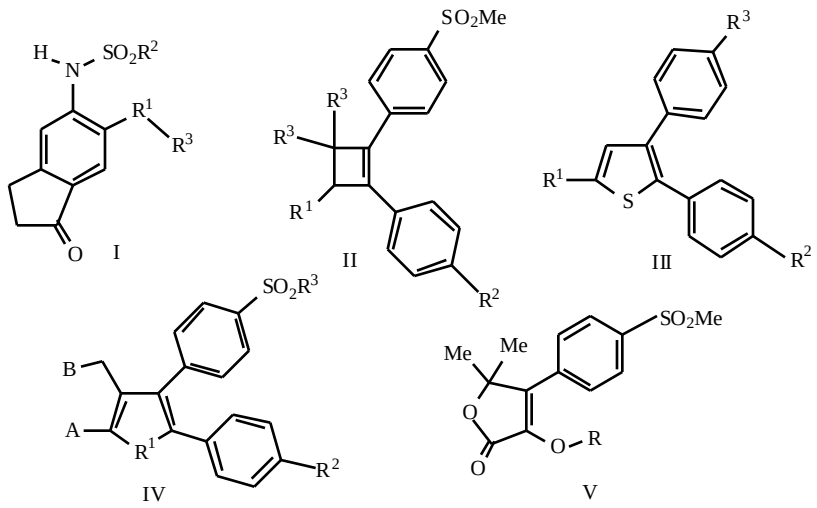

Fig. (3). Common molecular skeletons of the studied DS1-compounds (COX-2 inhibitors taken from different series).

Table 1. COX-2 Inhibition Indices IC_{50} (μM) and Substituents Related to the Structures by the Type I-IV

No. com	R1	R2	R3	IC_{50}	Exp	No. com	R1	R2	R3	IC_{50}	Exp
structures by the type I											
1	S	Me	2,4-Cl_2-Ph	0.01	+	14	S	Me	3-Me-Ph	>10	–
2	O	Me	2,4-F_2-Ph	0.021	+	15	S	Me	4-i-Pro-Ph	>10	–
3	S	Me	2,4-F_2-Ph	0.023	+	16	S	Me	4-t-Bu-Ph	>10	–
4	O	CF_3	2,4-F_2-Ph	0.04	+	17	S	Me	4-MeO-Ph	>10	–
5	S	Me	4-Me-Ph	0.05	+	18	O	Me	4-SO_2Me-Ph	>10	–
6	O	Me	Cyclohexyl	0.05	+	19	S	Me	4-CO_2H	>10	–
7	S	Me	Cyclohexyl	0.05	+	20	O	Me	4-thiazolyl	>10	–
8	S	Me	2-F-Ph	0.1	+	21	S	Me	5-thiazolyl	>10	–
9	S	Me	4-Et-Ph	0.1	+	22	O	Me	4-tetrahydro –pyranyl	>10	–
10	O	Me	4-SMe-Ph	0.1	+						
11	S	Me	2-thiazolyl	0.1	+	23	SO_2	Me	2,4-F_2-Ph	>10	–
12	CH_2	Me	2,4-F_2-Ph	0.2	+	24	S	Et	2,4-F_2-Ph	>10	–
13	S	Me	3-F-Ph	>10	–	25	S	COMe	2,4-F_2-Ph	>10	–
structures by the type II											
26	=CH_2	H	H	0.0012	+	30	O	H	-CH=CH-	0.012	+
27	=CH_2	H	Me	0.0022	+	31	NOH	H	Me	0.061	+
28	O	H	Me	0.0028	+	32	O	4-SO_2Me	Me	0.096	+
29	O	4-F	Me	0.0050	+	33	O	H	Me	0.110	+
structures by the type III											
34	Br	F	SO_2Me	0.005	+	43	H	F	COMe	>30	–
35	i-Pro	F	SO_2NH_2	0.010	+	44	H	F	OCOH	>30	–
36	H	F	SO_2NH_2	0.030	+	45	H	F	OCOMe	>30	–
37	MeOCO F		SO_2NH_2	0.070	+	46	H	F	CH_2OCOH	>30	–
38	H	F	SO_2NHMe	7.200	+	47	H	F	CHO	>30	–
39	H	F	SO_2Et	>30	–	48	H	F	CN	>30	–
40	H	CMe_2OH	SO_2NH_2	>30	–	49	H	F	CH_2OH	>30	–
41	MeOCO	SO_2NH_2	F	>30	–	50	H	F	SMe	>30	–
42	H	F	$CONH_2$	>30	–	51	H	F	SOMe	>30	–

structures by the type IV*													
No.com	**R1**	**R2**	**R3**	**A—B-**	**IC_{50}**	**Exp**	**No.com**	**R1**	**R2**	**R3**	**A—B**	**IC_{50}**	**Exp**
52	S	3,4-F_2	NH_2	CO-O-	98	+	57	S	3,4-F_2	Me	-CO-O-	64	+
53	O	H	Me	-C_3H_3-	94	+	58	NH	4-F	Me	-C_3H_3-	58	+
54	NH	SO_2Me	F#	-C_3H_3-	86	+	59	S	4-F	Me	-CO-O-	50	–
55	C=O	H	Me	-C_3H_3-	80	+	60	S	4-F	NH_2	-CO-O-	42	–
56	S	H	Me-CH-O-CO-		65	+	61	C=O	H	Me	-C_3H_3-	<17	–

* - IC_{50} in %
\# - SO_2R_3 substitued by F

Table 2. COX-2 Inhibition Indices IC_{50} (μM) and Substituents Related to the Structures by the Type V

No. comp	R	IC_{50}	No. comp	R	IC_{50}
62	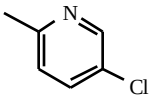	<0.01	73	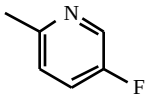	0.08
63	4-Cl-Ph	0.02	74	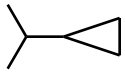	0.08
64	Ph	0.04			
65	2,4-F_2-Ph	0.04			
66	4-Me-Ph	0.04	75	2-Me-Ph	0.10
67	Cyclohexyl	0.04			
68		0.04	76	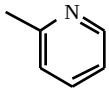	0.12
69	4-F-Ph	0.05	77	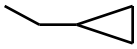	0.14
70	3,4-F_2-Ph	0.06			
71	3-F-Ph	0.07			
72	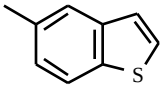	0.08	78	Et	23
			79	Me	33

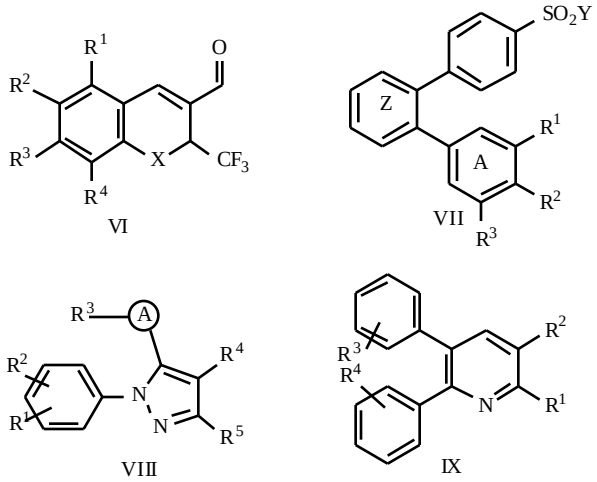

Fig. (4). Common molecular skeletons of the studied DS2-compounds: VI – benzopirane derivatives; VII – sulfonyl-contained terpenils; VIII – diaryl derivatives of pyrazole; IX – diaryl-substituted pyridines.

RESULTS AND DISCUSSION

a) Analysis of Pharmacophores and Antipharmacophores

Conformational analysis for all compounds was done by means of a molecular mechanics method (MMX) [61]. Their electronic structures were calculated from the semi-empirical AM1 method [62]. Conformational analysis shows that phenyl and benzene cycle planes are oriented by 33° to each other; sulfone group has a valance angle OSO equal to 115°; methyl sulfone fragment has the angle of 80.5° relative to the plane of benzene cycle. All this is in agreement with the data obtained from molecular docking and Monte Carlo simulations [4]. The results of conformational analysis and quantum-chemistry calculations were used to form ETMCs for all compounds. Charges on atoms (q_i) were selected as diagonal elements; the Wiberg's indices (W_{ij}) were taken as off-diagonal elements for chemically bonded atoms; otherwise, optimized distances between corresponding two atoms (R_{ij}) were used.

After processing the ETMCs, a set of pharmacophores ('activity features') was obtained. The features formed a basis for a system capable of carrying out computer screening and forecasting activities of new drug prototypes. Optimal values of variations allowable in the process of the matrices comparison (when testing if atoms and bonds match) were found as $\Delta_1=\pm0.12$ for diagonal elements (q_i) and $\Delta_2=\pm0.22$ for off-diagonal values (W_{ij} and R_{ij}). To determine the most informative activity features, the desired values of probabilistic estimations α_a and P_a were set as 0.50 and 0.80, correspondingly.

The set of selected pharmacophores formed the basis of a system for the COX-2 inhibitory activity prediction.

C1	C2	C3	C4	C8	C9	C10	S17	O18	O19	C20
-0.01	1.47	2.42	2.77	6.27	5.00	5.26	9.32	10.22	9.62	9.86
	0.01	1.44	2.40	7.44	6.10	6.11	10.14	11.15	10.31	10.60
		0.01	1.44	7.56	6.16	5.86	9.74	10.87	9.77	10.10
			0.01	6.54	5.14	4.66	8.42	9.59	8.44	8.73
				0.02	1.38	2.38	4.08	4.40	4.99	5.03
					0.06	1.39	4.65	5.31	5.29	5.48
						0.02	4.08	5.06	4.42	4.89
							0.96	0.85	0.85	0.93
								-0.49	2.44	2.59
									-0.49	2.59
										-0.11

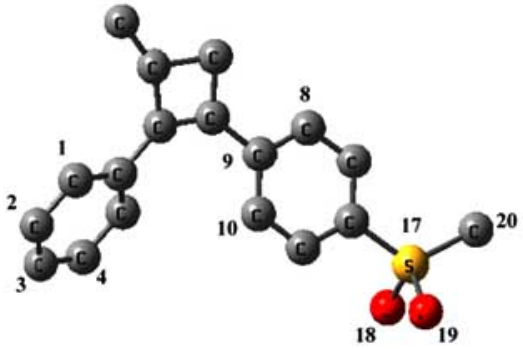

Fig. (5). Submatrix and corresponding structure of the Ph1 pharmacophore (obtained relative the template active compound **26**).

Compound **26** possessing the highest anti-inflammatory activity (i.e. as compound with the highest value of IC_{50} on COX-2) and a good selectivity index (IC_{50} on COX-2 is 450 times greater than IC_{50} on COX-1) was taken as a template for comparison. In Fig. **5**, a sub-matrix of the template ETMC (in short, its ETSC**)** is given, which corresponds to one of the pharmacophores (Ph1) revealed.

The given Ph1 pharmacophore consists of 11 atoms located in different parts of a molecule. Ph1 is found in 41 active and 6 inactive compounds. Probability of its realization P_a is 0.86. Sulfur atom S_{17} has a high positive charge q= 0.96e; negative charges are concentrated on atoms O_{18} and O_{19} of oxygen (q= -0.49e) and on the carbon atom of methylsulfone group (q= -0.11e). On the carbon atoms of phenyl groups ($C_1 \div C_4$ and $C_8 \div C_{10}$) charges are close to zero.

Docking of the celecoxib analogs into the COX-2 enzyme pointed out that just these parts of active molecules had played the most important role in the ligand-receptor binding (see for the enzyme crystal structure the Protein Data Bank, www.rcsb.org, the 6COX code). 5-Aryl ring of celecoxib makes hydrophobic contacts with Phe^{381}, Tyr^{385}, Phe^{513}, Trp^{387} and Leu^{384}. Sulfonyl atoms of oxygen make favorable electrostatic contact with Arg^{513} and Phe^{518} (i.e. each oxygen is capable of forming an O…H – N hydrogen bond). The Ph1 is very sensitive to different replacements

C12	C10	C5	C6	S22	O24	O23	C25
-0.09	2.55	4.48	5.06	9.20	10.42	9.42	9.96
	-0.05	5.00	4.64	8.38	9.39	8.33	8.84
		-0.03	1.46	4.85	5.24	5.50	5.66
			0.14	3.96	5.00	4.61	4.74
				1.04	0.87	0.87	0.94
					-0.49	2.44	2.64
						-0.49	2.58
							-0.13

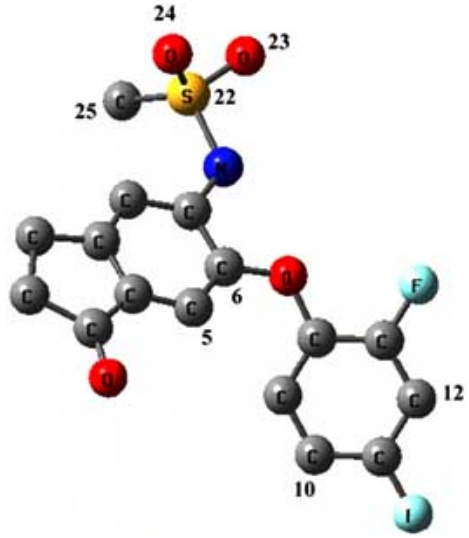

Fig. (6). Submatrix and corresponding structure of the Ph2 pharmacophore (obtained relative the template active compound **2**).

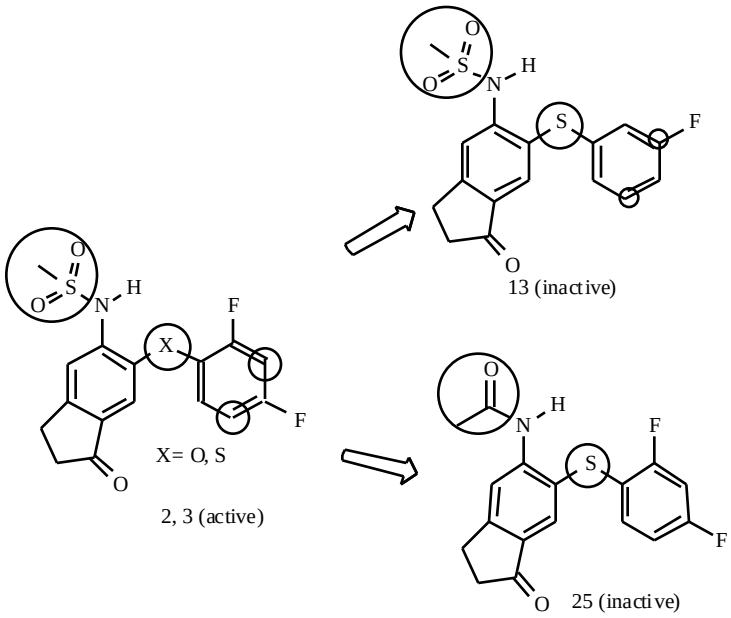

Fig. (7). Influence of atoms rearrangement and group replacement on the COX-2 inhibitory activity in the structures by the type I.

done in the phenyl ring. A substituent change, as well as any changes in the nature of its atoms, can cause the electron density redistribution in the investigated compound. As a consequence, the ETSC of the activity fragment can change considerably. From the example of group I it is seen how the activity feature given classifies compounds of the group into classes of activity. Compound **2** (see Table **1**) is considered as an active one (IC_{50} = 0.02-0.03 μM). It has 2,4-difluorophenyl as a substituent by the atom of oxygen from the ether group. A pharmacophore Ph2 found relative to compound **2** (template compound) is shown along with its ETSC in (Fig. **6**).

The Ph2 pharmacophore contains fewer atoms than Ph1, although methylsulfon part of the molecule is present again. Attention should be paid to atoms C_{10} and C_{12} of 2,4-difluorophenyl that enter the Ph2. Namely their positions are the most sensitive ones as to exhibiting the activity in view. In the case of 3-fluorophenyl as a substituent (compound **13**) and under condition that the rest of the molecular structure does not change, a sharp decrease of activity is observed (IC_{50}>10 μM). The system of the COX-2 inhibitory activity prediction classifies compound **13** as inactive, because its submatrix differs from the ETSC of the activity feature. The oxygen of the ether group replacement by sulfur (compound **3**) does not cause any activity changes (see Fig. **7**).

However, if methylsulfone is replaced (as in compound **2**) by acetyl in the 2,4-difluorphenyl presence (compound **25**), this causes decrease of inhibitory activity (IC_{50} of compound **25** is higher than 10 μM). At last, this pharmacophore does not enter compound **25** as a substructure. Therefore, this compound was not classified as an active one. Further, the pharmacophore Ph2 is realized in compound **68** (atoms entering the structural fragment are shown by dotted line in Fig. **8**). The i-Bu substituent replaced by Et (compound **78**) causes only partial presence of the structural feature. As a result, compound **78** does not possess inhibitory activity (IC_{50} = 23 μM).

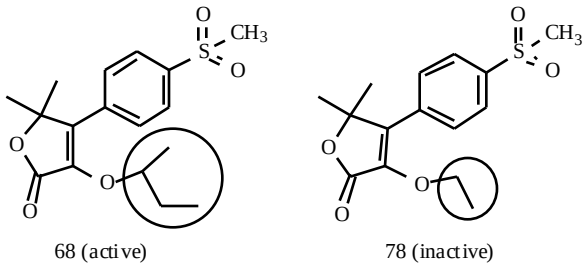

Fig. (8). Dependence of the COX-2 inhibitory activity on the R2 subsituent in the structures by the type II.

As mentioned before, compounds with distinct skeletons were selected for initial series to reveal best matching pharmacophores. The developed system for the activity prognostication classifies all five series of compounds well enough. It can be seen from the statistical estimates of the frequency of the pharmacophore Ph2 (Fig. **6**) occurrence in a series, which were calculated for all five series mentioned. Figure **9** illustrates the dependencies between average frequencies calculated for active and inactive compounds in each of the five mentioned series (i.e. the dependencies between frequencies and types of skeletons).

From Figure **9** it follows that the highest frequency of the pharmacophore appearance is reached in the group III. The frequency decreases in groups of compounds taken in the order V → I → IV and has the minimal value for the group IV. It can be explained by low values of inhibitory activity in this group. It should be noted, however, that the most active compounds from this group (see Table **4**) were classified by our system for COX-2 inhibitory activity prediction correctly. To check the ability of the obtained system to predict the activity correctly for skeletons that differ from the studied ones, the system was applied to structures being indomethacyne derivatives [63, 64] (see Fig. **10**).

A peculiarity of the compounds is that they have no sulfone group. However, our system classified them

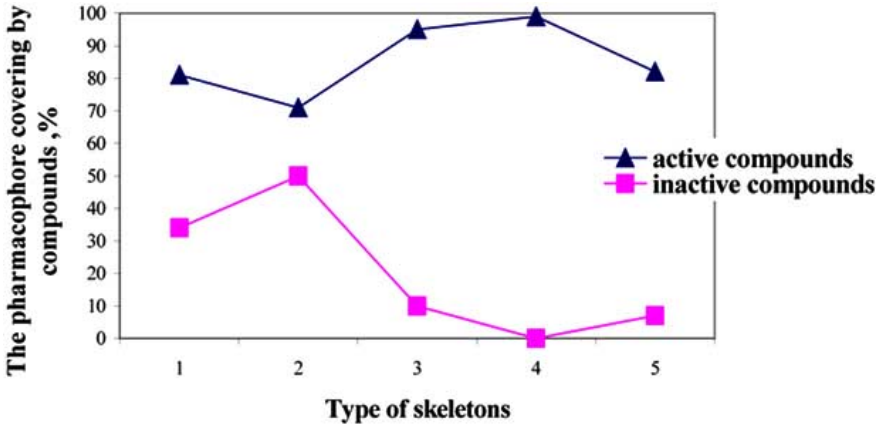

Fig. (9). Dependence of the pharmacophore Ph2 realization in the DS1 data set (5 series) on the type of the compounds skeletons.

correctly as active/inactive ones. In spite of the common structural similarity of the compounds, the R substituent's replacement in one of them causes considerable changes (loss/appearance) in the activity of the resulting compound, due to changes in its electronic-topological characteristics. Compound **80** has IC_{50}=0.3 nM, while compound **81** inhibits COX-2 by 1% under dosage of 100 nM. The result of the prognostication shows that active compound **80** possesses the found pharmacophore, while compound **81** does not possess it. By this, the ETSC of compound **80** consists of 9 atoms. Correspondence of the ETSC to one of pharmacophores found relative to the template compound **26** is shown in (Fig. **11**).

The most part of NSAIDs, which did not enter the teaching selection, were tested by means of the system developed for the COX-2 inhibitory activity prediction as well. (All these compounds passed pre-clinical and clinical trials.). The prognostication system recognized 95% of them as highly active compounds. In this way, the present study resulted in a system development that is capable of predicting the COX-2 inhibitory activity, which can be successfully used for carrying out computer screening and synthesis of potent inhibitors of COX-2 with diverse enough molecular skeletons.

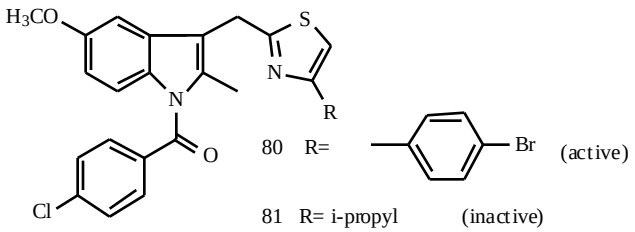

Fig. (10). Representatives of the examining selection being indomethacyne derivatives (compounds **80**, **81**).

b) Results of the ETM-NN Approach Application

The first stage of the data analysis was in finding a model of cluster distribution capable of reflecting the realistic internal structure of the data; the results are given in Table **3**. For the DS1, 337 clusters were found. ASNNs

C1	C2	C3	C4	C8	C9	C10	C16	C20*
C13	C9	C10	C12	C21	C22	C23	C19	Br27**
0.03	1.25	2.56	2.95	6.12	4.87	5.14	4.30	9.91
	0.02	1.60	2.54	7.64	5.92	6.05	5.76	9.85
		0.07	1.25	7.76	6.24	5.67	6.06	9.89
			-0.02	6.39	4.92	4.61	5.95	8.58
				0.01	1.40	2.40	3.02	5.18
					0.02	1.39	2.52	5.70
						0.02	3.76	4.83
							-0.07	8.10
								-0.20

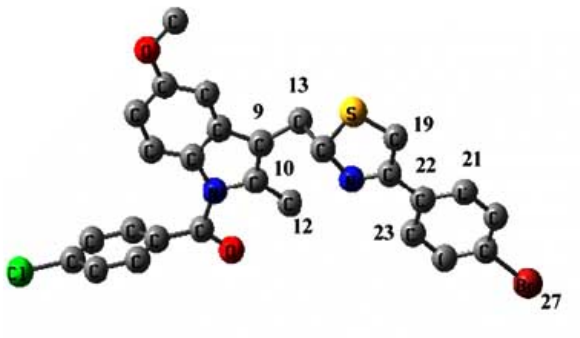

*atoms' numeration in the template compound **26**
** atoms' numeration in compound **80**

Fig. (11). The Ph3 activity fragment and its correspondent submatrix (obtained from the template active compound **80**).

recognized correctly 87.4%, or 59 from 68 compounds, while for the test set the result was a bit lower, i.e. 81.8%, or 9 compounds from 11. For the summary set the result equals to 87.7% (70 compounds from 79).

Table 3. Results of the Data on the COX –2 Inhibitors Clustering

N/N	Data	Clusters number	Molecules	
			in total	Number of predicted
Data set 1				
1	Training set	337	68	59(87.4%)
2	Test set	337	11	9(81.8%)
3	Total set	337	79	70(87.7%)
Data set 2				
1	Training set	385	205	192(93.7%)
2	Test set	385	22	17(77.3%)
3	Total set	385	227	214 (94.3%)

For the DS2 the results were, correspondingly, 93.7% for training set (192 compounds from 205), 77.3% for the test set (17 compounds from 22), and for the summary set ASNNs recognized correctly 94.3% or 214 compounds from 227. The results obtained tell in favor of high quality of models for cluster distribution and its fitness for the analysis of new data sets, so as for the search for pharmacophors.

At the second stage, only about 115 fragments were selected for the DS1 and 125 of them were selected for DS2 (see Table **4**). On the base of weights calculated for the molecular fragments represented by ETMSs, ASNN were capable of recognizing 80.6%, or 55 compounds from 68, as to the training set, and 90.9% or 10 compounds from 11, for the test set. In total, the network classified correctly 85.1% or 67 compounds from 79.

For the DS2, second data selection, the results were 87.3%, or 179 compounds from 205, for training set, and 81.8%, or 18 compounds from 22, for test set, correspondingly. For the summary data set the result was 89.9% (204 compounds from 227). The pruning methods application afforded the selection of only 17 the most influential ETMC fragments for the DS1. By this, ASNN classified correctly 84.5%, or 88 compounds from 103, for the training set, and 90.9%, or 10 compounds from 11, for the test set. As to the DS2, only 12 fragments from 125 were selected for the further use. ASNNs classified correctly 88.8% (182 compounds from 205) and 86.4% (19 compounds from 22) for training and test sets, correspondingly.

In our case, the two models comparison (one model based on the cluster distribution found in a straightforward manner, and another based on the ETMC fragments use for the network training) tells in favor of close correspondence between their results. However, the first model is not stable enough and depends severely on the structures of compounds selected for the training set. However, in comparison with other commonly used approaches, the approach presented in this study has shown quite satisfactory results. This fact tells about workability of the both models found. These models can be applied for new potent COX-2 inhibitors design.

CONCLUSION

Peculiarities of conformational and electronic structures belonging to a large series of COX-2 inhibitors were studied. The results of the study agree satisfactorily with data obtained by other researches relative to the same classes of compounds. By means of the ETM-software, SARs were studied in the series of COX-2 inhibitors possessing quite different skeletons.

A system for the COX-2 inhibitory activity prediction was developed on the base of the pharmacophores revealed. The obtained system allows for carrying out screening and design of potent COX-2 inhibitors. The results of the ETM

Table 4. Results Calculated for COX –2 Inhibitors After Training SOM with the Pharmacophores Data

N/N	Sets	All pharmacophores			Pharmacophores selected by pruning methods		
		Param. number	Molecule		Param. number	Molecule	
			in total	Predicted (%)		in total	Predicted (%)
Data set 1							
1	Training set	115	68	55 (80.6%)	17	68	59 (84.5%)
2	Test set	115	11	10 (90.9%)	17	11	10 (90.9%)
3	Total set	115	79	67 (85.1%)	17	79	69 (86.8%)
Data set 2							
1	Training set	125	205	179(87.3%)	12	205	182(88.8%)
2	Test set	125	22	18 (81.8%)	12	22	19(86.4%)
3	Total set	125	227	204 (89.9%)	12	227	205(90.3%)

application to the test selection have shown that 95% of the compounds are classified correctly.

ACKNOWLEDGEMENT

Gratitude is expressed to the TÜBİTAK organization (Turkey) from V.K. for the financial support.

REFERENCES

[1] Lombardino, G. *Nonsteroidal Anti-inflammatory Drugs*. Wiley Inter-Science, John Wiley & Sons: New York, 1985.

[2] Reitz, D.B.; Seibert, K. *Annu. Rep. Med. Chem*. **1995**, *30*, 179.

[3] Prasit, P.; Riendeau, D. *Annu. Rep. Med. Chem*. **1997**, *32*, 211.

[4] Filizola, M.; Perez, J.J.; Palomer, A.; Mauleon, D. *J. Mol. Graphics Mod*. **1997**, *15*, 290.

[5] Price, M. L. P.; Jorgensen, W. L. *J. Am. Chem. Soc.* **2000**, *122*, 9455.

[6] Reitz, D. B.; Isakson, P. C. *Curr. Pharm. Des.* **1995**, *1*, 211.

[7] Leval, X.; Delarge, J.; Somers, F.; Tullio, P.; Henrotin, Y.; Pirotte, B.; Dogne, J.-M. *Curr. Med. Chem.* **2000**, *7*, 1041.

[8] Moore, B. C.; Simmons, D. L. *Curr. Med. Chem*. **2000**, *7*, 1131.

[9] Soliva, R.; Almansa, C.; Kalko, S.G.; Luque, F. J.; Orozco, M. *J. Med. Chem.* **2003**, *46*, 1372.

[10] Garciya-Nieto, R.; Perez, C.; Gago, F. *J. Comp. Aid. Mol. Des.* **2000**, *14*, 147.

[11] Chakraborti, A. K.; Thilagavathi, R. *Bioorgan. Med. Chem*. **2003**, *11*, 3989.

[12] Chakraborti, A. K.; Thilagavathi, R. *Internet Electronic Journal of Molecular Design*, **2003**, 2. BioChem Press http://www.biochemp-ress.com

[13] Stahl, M.; Todorov, N. P.; James, T.; Mauser, H.; Boehm, H.-J.; Dean, P. M. *J. Comp.-Aided. Mol. Des.* **2002**, *16*, 459.

[14] Zhu, J.; Yu, H.; Fan, H.; Liu, H.; Shi, Y. *J. Comp.-Aided. Mol. Des*. **2001**, *15*, 447.

[15] Llorens, O.; Perez, J. J.; Palomer, A.; Mauleon, D. *J. Mol. Graph. Modell*. **2002**, *20*, 359.

[16] Arakawa, M.; Hasegawa, K.; Funatsu, K. *J. Chem. Inf. Comp. Sci*. **2003**, *43*, 1396.

[17] Almansa, C.; Alfón, J.; de Arriba, A. F.; Cavalcanti, F. L.; Escamilla, I.; Gómez, L. A.; Miralles, A.; Soliva, R.; Bartrolí, J.; Carceller, E.; Merlos, M.; García-Rafanell, J. *J. Med. Chem.* **2003**, *46*, 3463.

[18] Horng-Huey, Ko.; Tsao, Lo-Ti; Kun-Lung, Yu; Cheng-Tsung, Liu; Jih-Pyang, Wang; Chun-Nan, Lin. *Bioorg. Med. Chem*. **2003**, *11*, 105.

[19] Quintela, J. M.; Peinador, C.; González, L.; Devesa, I.; Ferrándiz, M. L.; Alcaraz, M. J.; Riguera, R. *Bioorg. Med. Chem*. **2003,** *11*, 863.

[20] Vigorita, M.G.; Ottaná, R.; Monforte, F.; Maccari, R.; Monforte, M.T.; Trovato, A.; Taviano, M.F.; Miceli, N.; De Luca, G.; Alcaro, S.; Ortuso, F. *Bioorg. Med. Chem*. **2003,** *11*, 999.

[21] Hashimoto, H.; Maeda, K.; Ozawa, K.; Haruta, J.; Wakitani, K. *Bioorg. Med. Chem. Lett.* **2002,** *12*, 65.

[22] Hu, W.; Guo, Z.; Yi, X.; Guo, C.; Chu, F.; Cheng, G. *Bioorg. Med. Chem.* **2003**, *11*, 5539.

[23] Rahim, M. A.; Rao, P. N. P.; Knaus, E. E. *Bioorg. Med. Chem. Lett.* **2002**, *12*, 2753.

[24] Paramashivappa, R.; Phani Kumar, P.; Subba Rao, P.V.; Srinivasa Rao, A. *Bioorg. Med. Chem. Lett.* **2003**, *13*, 657.

[25] Li, C. S.; Brideau, C.; Chan, C. C.; Savoie, C.; Claveau, D.; Charleson, S.; Gordon, R.; Greig, G.; Gauthier, J. Y.; Lau, C. K.; Riendeau, D.; Thérien, M.; Wong, E.; Prasit, P. *Bioorg. Med. Chem. Lett.* **2003**, *13*, 597.

[26] Haifeng Chen; Qiang Li; Xiaojun Yao; BoTao Fan; Shengang Yuan; Panayea, A.; Douceta, J. P. *QSAR* **2004**, *23*, 36.

[27] Jian-Xia Lü; Qi Shen; Jian-Hui Jiang; Guo-Li Shen; Ru-Qin Yu, J. *Pharm. Biomed. Analysis* **2004**, *35*, 679.

[28] Shahapurkar, S.; Pandya, T.; Kawathekar, N.; Chaturvedi, S.C.; *Eur. J. Med. Chem*. **2004,** *39*, 383.

[29] Hye-Jung Kim; Chong Hak Chae; Kyu Yang Yi; Kyung-Lae Park; Sung-eun Yoo; *Bioorg. Med. Chem*. **2004**, *12*, 1629.

[30] Shvets, N.M.; Dimoglo, A.S. *Nahrung.* **1998**, *42*, 364.

[31] Dimoglo, A.S.; Beda, A.A.; Shvets, N.M.; Gorbachov, M.Yu.; Kheifits, L.A.; Aulchenko, I.S. *New. J. Chem.* **1995**, *19*, 149.

[32] Dimoglo, A.S.; Vlad, P.F.; Shvets, N.M.; Coltsa, M.N. *New J. Chem*. **2001**, *25*, 283.

[33] Dimoglo, A.S.; Shvets, N.M.; Tetko, I.V.; Livingstone, D.J. *QSAR*, **2001**, *20*, 31.

[34] Dimoglo, A.S.; Chumakov, Yu.M.; Dobrova, B.N.; Shvets, N.M.; Saracoglu, M. *Arzneim.-Forsch./Drug Res*. **1997**, *47*(I), 415.

[35] Dimoglo, A.S.; Sim, E.P.; Shvets, N.M.; Ahsen, V. *Mini-Rev. Med. Chem*. **2003**, *3*, 293.

[36] Manallack, D. T.; Livingstone, D. J. *Eur. J. Med. Chem*. **1999**, *34*, 195.

[37] Zupan, J.; Gasteiger, J. *Neural Networks for Chemistry and Drug Design: An Introduction*; 2nd edition, VCH: Weinheim, **1999**.

[38] Tetko, I. V.; Luik, A. I.; Poda, G. I. *J. Med. Chem*. **1993**, *36*, 811.

[39] Dimoglo, A. S.; *Chim. Pharm. Zh. (Russ.)* **1985**, *19*, 438.

[40] Shvets, N.M. *Comp. Sci. J. Moldova* **1993**, *1*(3), 101.

[41] Shvets, N.M.;*Comp. Sci. J. Moldova* **1997**, *5*(3), 309.

[42] Shvets, N.M.; Terletskaya, A.; Dimoglo, A.S.; Chumakov, Yu, M. *THEOCHEM. (J. Mol. Str.)* **1999**, *463*, 105.

[43] Kohonen, T. *Self-organisation Maps*; Springer-Verlag: Berlin,1995.

[44] Simon, V.; Gasteiger, J.; Zupan, J. A. *J. Am. Chem. Soc.* **1993**, *115*, 9148.

[45] Tetko, I.V. *J. Chem. Inf. Comput. Sci.* **2002**, *42*, 717.

[46] Tetko I.V.; Kovalishyn V.V.; Livingstone D. J. *J. Med. Chem.* **2001**, *44*, 2411.

[47] Tetko, I. V.; Villa, A. E. P.; Livingstone, D. J. *J. Chem. Inf. Comput. Sci.* **1996**, *36*, 794.

[48] Kovalishyn, V. V.; Tetko, I. V.; Luik, A. I.; Kholodovych, V. V.; Villa, A. E. P.; Livingstone, D.J. *J. Chem. Inf. Comput. Sci.* **1998**, *38*, 651.

[49] Tetko, I. V.; Livingstone, D. J.; Luik, A. I. *J. Chem. Inf. Comput. Sci.* **1995**, *35*, 826.

[50] Li, C.-S.; Black, W.C.; Chan, C.C.; Ford-Hutchinson, A.W.; Gauthier, J.Y.; Gordon, R.; Guay, D.; Kargman, S.; Lau, C.K.; Manchini, J.; Ouimet, N.; Roy, P.; Vickers, P.; Wong, E.; Young, R.N.; Zamboni, R.; Prasit, P. *J. Med. Chem*. **1995**, *38*, 4897.

[51] Leblanc, Y.; Roy, P.; Boyce, S.; Brideau, C.; Chan, C.C.; Charleson, S.; Gordon, R.; Grimm, E.; Guay, J.; Leger, S.; Li, C.S.; Riendeau, D.; Visco, D.; Wang, Z.; Webb, J.; Xu, L.J.; Prasit, P. *Bioorg. & Med. Chem. Lett*. **1999**, *9*, 2207.

[52] Li, C.-S.; Black, W.C.; Brideau, C.; Chan, C.C.; Charleson, S.; Cromlish, W.A.; Claveau, D.; Gauthier, J.Y.; Gordon, R.; Greig, G.; Grimm, E.; Guay, J.; Lau, C.K.; Riendeau, D.; Therien, M.; Visco, D.M.; Wong, E.; Xu, L.; Prasit, P. *Bioorg. & Med. Chem. Lett.* **1999**, *9*, 3181.

[53] Lau, C. K.; Brideau, C.; Chan, C.C.; Charleson, S.; Cromlish, W.A.; Ethier, D.; Gauthier, J.Y.; Gordon, R.; Guay, J.; Kargman, S.; Li, C.-S.; Prasit, P.; Riendeau, D.; Therien, M.; Visco, D.M.; Xu, L. *Bioorg. & Med. Chem. Lett*. **1999**, *9*, 3187.

[54] Friesen, R. W.; Dube, D.; Fortin, R.; Frenette, R.; Prescott, S.; Cromlish, W.; Greig, G.M.; Kargman, S.; Wong, E.; Chan, C.C.; Gordon, R.; Xu, L.J.; Riendeau, D. *Bioorg. Med. Chem. Lett.* **1996**, *6*, 2677.

[55] Leblanc, Y.; Gauthier, J.Y;. Ethier, D.; Guay, J.; Manchini, J.; Riendeau, D.; Tagari, P.; Vickers, P.; Wong, E.; Prasit, P. *Bioorg. & Med. Chem. Lett*. **1995**, *5*, 2123.

[56] Prasit, P.; Guay, D.; Wang, Z.; Leger, S.; Therien, M. *Pat.US*, **1996**, 5.521.213.

[57] Carter, J.S.; Obukowicz, M.J.; Davedas, B.; Talley, J.J.; Brown, D.L.; Graneto, M.J.; Bertenshaw, S.R.; Rogier, J.D.J.; Nagarajan, S.R.; Hanau, C.E.; Hartman, S.J.; Ludwig, C.L.; Metz, S. *US Patent* **2000**, 6.034.256.

[58] Li, J.J.; Norton, M.B.; Reinhard, E.J.; Anderson, G.D.; Gregory, S.A.; Isakson, P.C.; Coboldt, C.M.; Masferrer, J.L.; Perkins, W.E.; Seibert, K.; Zhang, Y.; Zweifel, S.; Reitz, D.B. *J. Med. Chem.* **1996**, *39*, 1846.

[59] Penning, T.D.; Talley, J.J.; Bertenshaw, S.R.; Carter, J.S.; Collins, P.W.; Docter, S.; Graneto, M.J.; Lee, L.F.; Malecha, J.W.; Miyashiro, J.M.; Rogers, R.S.; Rogier, D.J.; Yu, S.S.; Anderson, G.D.; Burton, E.G.; Cogburn, J.N.; Gregory, S.A.; Koboldt, C.M.; Perkins, W.E.; Seibert, K.; Veenhuizen, A.W.; Zhang, Y.Y.; Isakson, P.C. *J. Med. Chem.* **1997**, *40*, 1347.

[60] Weier, R.M.; Lee, L.F.; Partis, R.A.; Koszyk, F.J. *US Patent* **1999**, 5.916.905.

[61] Gilbert, K.; Gaevski, J. A. *MMPi Molecular Mechanics* Program, Indiana University, Indiana, 1985.
[62] Dewar, M.J.S.; Zoebisch, E.G.; Healy E.F.; Stewart, J.J.P. *J. Am. Chem. Soc*. **1985**, *107*, 3902.
[63] Woods, K.W.; McCroskey, R.W.; Michaelides, M.R.; Wada, C.K.; Hulkower, K.I.; Bell, R.L. *Bioorg. & Med. Chem. Lett*. **2001**, *11*, 1325.
[64] Danhardt, G.; Laufer, S. *Curr. Med. Chem*. **2000**, *7*, 1101.